Hindawi Publishing Corporation
Advances in Materials Science and Engineering
Volume 2015, Article ID 309135, 11 pages
http://dx.doi.org/10.1155/2015/309135

Research Article

Shear Failure of RC Dapped-End Beams

Muhammad Aswin,[1] Bashar S. Mohammed,[1] M. S. Liew,[1] and Zubair Imam Syed[2]

[1]*Department of Civil and Environmental Engineering, Universiti Teknologi PETRONAS, 32610 Bandar Seri Iskandar, Perak Darul Ridzuan, Malaysia*
[2]*Department of Civil Engineering, Abu Dhabi University, P.O. Box 59911, Abu Dhabi, UAE*

Correspondence should be addressed to Muhammad Aswin; aswin_tekniksipil@yahoo.com

Received 2 May 2015; Revised 6 August 2015; Accepted 6 August 2015

Academic Editor: João M. P. Q. Delgado

Reinforced concrete dapped-end beams (RC-DEBs) are mainly used for precast element construction. RC-DEBs generally are recessed at their end parts and supported by columns, cantilevers, inverted T-beams, or corbels. The geometric discontinuity of dapped-end beams evokes a severe stress concentration at reentrant corners that may lead to shear failure. Therefore, stress analysis is required at the reentrant vicinity for design requirement of these beams. Four large-scale RC-DEBs specimens were prepared, cast, and tested up to failure. Three parameters were investigated: amount of nib reinforcements, main flexural reinforcements, and concrete type at the dapped-end area. Finite element analysis using Vec2 was also conducted to predict the behavior of RC-DEBs. It has been found that highest stresses concentration factors occur at the reentrant corners and its vicinity. By using engineered cementitious composite (ECC) in the dapped-end area, the failure load has increased by 51.9%, while the increment in the failure load was 62.2% and 46.7% as the amount of nib reinforcement and main flexural reinforcement increased, respectively. In addition, Vec2 analysis has been found to provide better accuracy for predicting the failure load of RC-DEBs compared to other analysis approaches.

1. Introduction

The reinforced concrete dapped-end beams (RC-DEBs) are usually used for precast elements construction of bridge girders [1]. RC-DEBs are recessed at end parts and supported by columns, cantilevers, inverted T-beams, or corbels. The advantages of using these beams are, firstly, to increase the lateral stability of the structure elements at the support and, secondly, to decrease the overall height of the precast concrete floor [2, 3]. However, due to recessing of RC beam at end parts, there are two main problems related to designing RC-DEBs. Firstly, if the nib section height is less than 0.45 times total height of the beam (undapped section) then the beams exhibit a very small shear strength capacity. According to Wang et al. [4], it was recommended that the nib height should not be less than 0.45 times total beam height which is in agreement with the suggestion by Mattock and Chan [5]. Secondly, the geometric discontinuity leads to high stress concentrations at the reentrant corners. If appropriate reinforcements are not prepared close to reentrant corner, diagonal cracks can appear rapidly and failure can occur immediately or without early warning [6]. Strut-and-Tie Models are widely used in analysis of RC-DEBs and many models available in the codes of practice (such as ACI code, FIP, Eurocode2, Canadian code) which can provide significantly different results for the same specimen. This condition can be attributed to the use of different truss model to capture the stress flow at the dapped-end area.

Based on available experimental results, the failure of RC-DEBs commonly occurs at the reentrant corners or dapped-end area. The applied load is usually positioned at a distance in which shear span-depth ratio (a_v/d) is less than 2, where a_v is the shear span (distance from the load point to the support) and d is the effective depth of RC-DEB. However, limited research works have been carried out to determine the structural behavior of the RC-DEBs. Yang et al. [7] investigated the shear strength of RC-DEBs using failure mechanism or yield line theorem and found that their proposed analysis provides adequate predicted shear strength. Lu et al. [3] have experimentally investigated the shear strength capacity

of the RC-DEBs and they reported that the shear strength of dapped-end beams increases with increase of concrete compressive strength and nib flexural reinforcement area. The shear strength capacity of RC-DEBs also increases with decrease of nominal shear span-depth ratio. Mattock [8] demonstrated that dapped-end beams exhibit different shear capacity with variation of the nib height and nominal shear span-depth ratio, while Peng [9] suggested that, by using a proper anchorage and adequate hanger reinforcements, RC-DEBs exhibit higher shear strength capacity and good ductility even after yielding of hanger reinforcements. Wang et al. [4] have showed that the shear strength capacity of RC-DEBs is enhanced by increasing the nib height, nominal shear span, or amount of hanger reinforcements. It was also noted that, by using diagonal reinforcement through the reentrant corners, shear strength capacity can be increased.

Different strengthening techniques have been employed to enhance the shear strength capacity of RC-DEBs such as the use of external steel angle, unbounded inclined steel bolts, steel plate jacketing, and CFRP [1]. It has been reported that all the strengthening methods are enhancing the shear strength capacity of RC-DEBs; however, the unbounded inclined steel bolts method has yielded better results. In addition, experimental results reported by Huang and Nanni [6] and Nagy-György et al. [10] showed that the shear strength capacity of the RC-DEBs can be significantly increased by using CFRP strengthening. Other approaches by focusing on different types of concrete to enhance the shear strength capacity of RC-DEBs have been investigated by Mohamed and Elliot [11]. They investigated the shear capacity of RC-DEBs made of self-compacting steel fiber concrete and reported that the shear capacity has been enhanced, which can lead to reduction in the amount of dapped-end reinforcements.

Fukuyama et al. [12] reported that a new ductile engineered cementitious composite (ECC) has been developed based on the micromechanical principles by V. C. Li. The ECC mixtures exhibit wide range of strain hardening with up to 7% strain capacity and show steel-like behavior. Further details on ECC properties and behavior have been reported by other researchers [13–18].

Therefore, the main objective of the research work reported in this paper is to predict the failure load and load-deformation response of RC-DEBs, as well as to investigate the stress concentration at the dapped-end area. Three parameters were considered: concrete type at the nib area, amount of nib reinforcement, and amount of main flexural reinforcement. In this study, the steel reinforcements requirement of RC-DEBs were designed using the PCI Design Handbook [19], whereas the failure load of RC-DEBs was predicted using available codes, Strut-and-Tie Model (STM), and finite element modeling (FEM). All these analysis results were compared to experimental results to gain the accurate analysis.

2. Experimental Works

For this study, four large-scale RC-DEBs were prepared and cast in accordance with the requirements of PCI code. All beams were tested up to failure.

Table 1: Mix proportions.

Ingredients	NSC	ECC
Cement (OPC)	1.00	1.00
Fly ash	—	1.20
Water	0.57	0.32
Fine aggregate	1.64	0.80
Coarse aggregate	2.00	—
Superplasticizer	—	1%
PVA fiber	—	2%

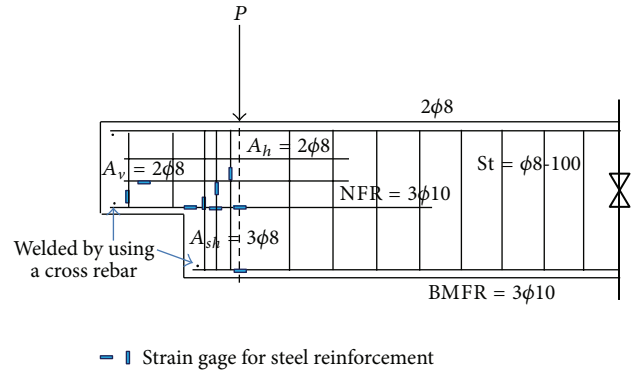

Figure 1: Reinforcement details.

2.1. Test Specimens. The overall length of each RC-DEB was 1800 mm. The nib dimensions were 110 mm length, 140 mm height, and 120 mm width. The undapped portion dimensions were 120 mm width and 250 mm height. The beams were labeled as DEB-1, DEB-2, DEB-3, and DEB-4. Normal strength concrete (NSC) was used in DEB-1, DEB-3 and DEB-4. While ECC mixture was used only in the dapped-end area of DEB-2. Only longitudinal reinforcement was used (without shear reinforcement) for DEB-1 and DEB-2. Steel reinforcement for DEB-3 and DEB-4 was in accordance with the requirements of PCI code. However, main flexural reinforcement for DEB-4 was decreased by 36%. The mix proportions for normal concrete and ECC are shown in Table 1. Concrete cover of 15 mm is provided for all reinforcement bars. NSC and ECC compressive strength and the reinforcement details are shown in Table 2 and Figure 1. All main longitudinal reinforcements either in extended end or undepth portion of beams were welded at the ends of the beams using cross steel bars to provide sufficient anchorage in accordance with the requirements of ACI code [22] as shown in Figure 1.

2.2. Instrumentations. All beams were tested with nominal shear span (a) of 102 mm and nib depth (d) of 112 mm. The selected nominal shear span-depth ratio (a/d) was 0.91 (less than 1) to fulfill the PCI requirements. Four rosette strain gages were attached to the surface of each beam to study the principal stresses and stress concentration at points A, B, C, and D as shown in Figure 2. Uniaxial strain gages were attached to main flexural reinforcement, nib flexural reinforcement, and hanger reinforcement as well as nib

Table 2: The compressive strength and reinforcement details.

Specimen	f_c' MPa	Concrete type	A_h mm	A_v mm	HR mm	f_{ys} MPa	NFR mm	BMFR mm	f_y MPa
DEB-1	27	NSC	—	—	—		3ϕ10	3ϕ10	470
DEB-2	27; 79	NSC; ECC	—	—	—		3ϕ10	3ϕ10	
DEB-3	27	NSC	2ϕ8 (U)	2ϕ8 (St)	3ϕ8 (St)	387	3ϕ10	3ϕ10	
DEB-4	27	NSC	2ϕ8 (U)	2ϕ8 (St)	3ϕ8 (St)		3ϕ10	3ϕ8	

U = U bar (2 legs); St = stirrup (2 legs); A_h = nib horizontal reinforcement, A_v = nib vertical reinforcement; HR = A_{sh} = hanger reinforcement; NFR = nib flexure reinforcement; BMFR = beam main flexure reinforcement; f_c' = concrete compressive strength; and f_y = yield stress of reinforcement.

Table 3: Experimental and analysis results.

Number	Failure load (kN)				Failure load ratio (analysis-experimental)		
	Test P_u^E	PC P_u^{PC}	STM P_u^{STM}	Vec2 P_u^{Vec2}	P_u^{PC}/P_u^E	P_u^{STM}/P_u^E	P_u^{Vec2}/P_u^E
DEB-1	64.87	56.25	96.34	58.00	0.87	1.49	0.89
DEB-2	98.56	83.27	96.34	95.80	0.84	0.98	0.97
DEB-3	105.26	96.67	96.34	107.80	0.92	0.92	1.02
DEB-4	95.16	96.67	50.71	107.00	1.02	0.53	1.12
Mean (M)					0.91	0.98	1.00
Standard deviation (S)					0.05	0.34	0.09
Coefficient of variation (CoV)					0.06	0.35	0.08

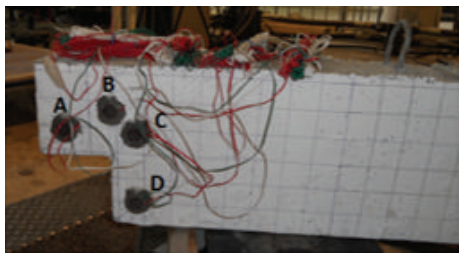

Figure 2: Layout of the rosette strain gages.

vertical and horizontal reinforcement to evaluate the strains values in these reinforcements as shown in Figure 1. Linear Variable Differential Transducer (LVDT) was positioned at the soffit of the beam below the loading point to measure the vertical deflection. The test setup of the beams is shown in Figures 3(a) and 3(b). To study the localized effect of shear failure of the RC-DEBs, the shear span-depth ratio (a_v/d) was taken as 1.43 (less than 2).

3. Results and Discussion

3.1. Failure Load. The failure loads for all RC-DEBs are shown in Table 3. Different analytical methods were used to predict the failure load of RC-DEBs. To explore the accuracy of analytical methods, the analytical results were compared to the experimental results. Analytical results based on available codes are labeled as P^C. Results from Strut-and-Tie Model were labeled as P^{STM} and lastly, results from finite element modeling by package Vector2 were grouped and labeled as P^{Vec2}. In first group (P^C): DEB-1 was analyzed according to ACI code [22] for singly reinforced concrete without stirrups, DEB-2 was analyzed according to RILEM provision for fiber reinforced concrete [20, 21], and DEB-3 and DEB-4 was analyzed according to Section 5.6.3 of PCI code. It is worth noting that no single code is suitable for analyzing all the beams; therefore three codes were used in the analysis.

Stress-strain relationship of steel fiber reinforced concrete with ordinary reinforcing bars based on RILEM provision is shown in Figure 4.

According to Figure 4,

$$M_n = A_s f_y \left(d - \frac{a}{2}\right) + f_{ft}\,(h - x)\,bz, \tag{1}$$

where A_s and f_y are area and yield strength of steel reinforcements, respectively, $F_{fc,t} = f_{ft}(h-x)b$ is tensile force of fiber reinforced concrete, $f_{ft} = 0.33\sqrt{f_{ct}'}$ is tensile strength of concrete [23], f_{ct}' is compressive strength of concrete, $z = 0.5(h - x) + x(1 - \beta_1/2)$ is internal lever arm, h is total height of beam, d is effective depth, x is neutral axis position measured from the top of beam, c is distance between center of flexure rebar and bottom side of beam, β_1 is coefficient of compressive stress block, $a = \beta_1 x$, and b is width of beam.

Five potential failure modes of RC dapped-end beam are suggested by PCI code as shown in Figure 5. These failure

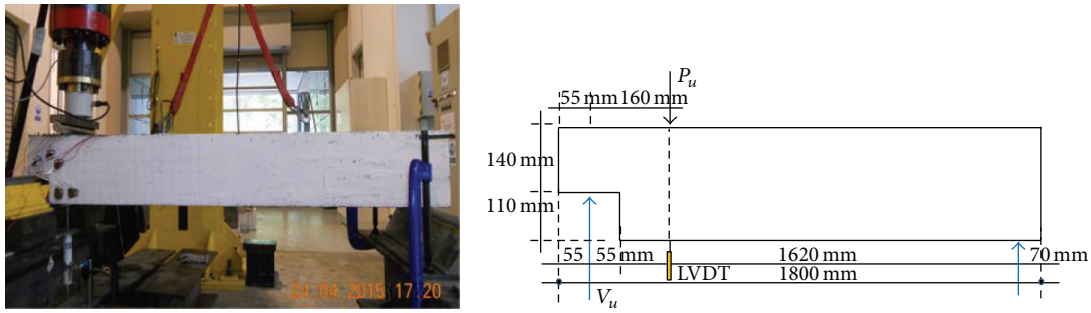

Figure 3: Experimental setup.

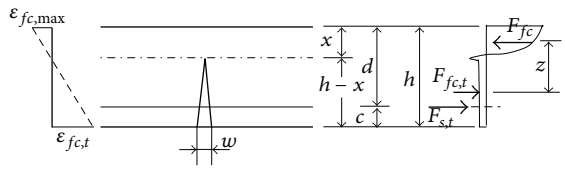

Figure 4: The stress-strain relationship, RILEM [20, 21].

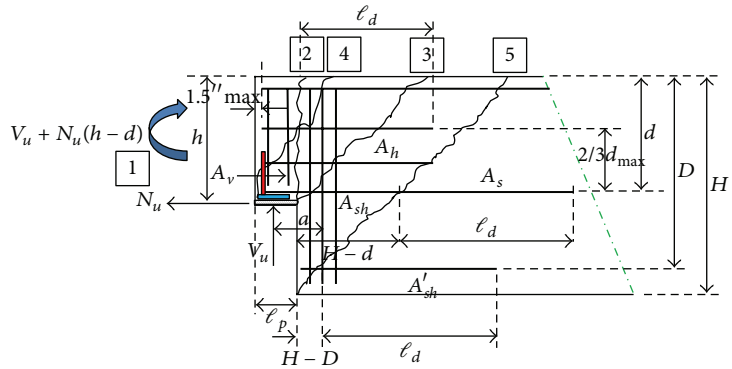

Figure 5: Potential failure modes [19].

modes are (1) flexure and axial tension in extended end, (2) direct vertical shear between nib and undapped portion, (3) diagonal tension initiating from reentrant corner, (4) diagonal tension in the nib area, and (5) diagonal tension in undapped portion. According to the empirical method specified in the PCI code, the smallest value of strength capacity which was calculated is taken as the predicted failure load of RC dapped-end beams:

(1) the flexure and axial tension in the nib

$$A_s = \frac{\left[V_u\,(a/d) + N_u\,(h/d)\right]}{\varphi f_y}, \tag{2}$$

where V_u = reaction force; φ = strength reduction factor = 0.75; and $N_u = 0$ (no bearing pad),

(2) direct shear

$$A_s = \frac{(2V_u)}{(3\varphi f_y \mu_e)} + \frac{N_u}{(\varphi f_y)}, \qquad \mu_e = \frac{(1000\varphi\lambda b h \mu)}{V_u}, \tag{3}$$

where $\mu_e \le 3.4$; λ = concrete coefficient = 1 for normal weight; μ = shear-friction coefficient = $1.4 * \lambda$,

(3) hanger reinforcement for diagonal tension at reentrant corner

$$A_{sh} = \frac{V_u}{(\varphi f_{yp})}, \tag{4}$$

where f_{yp} = the yield stress of hanger reinforcement,

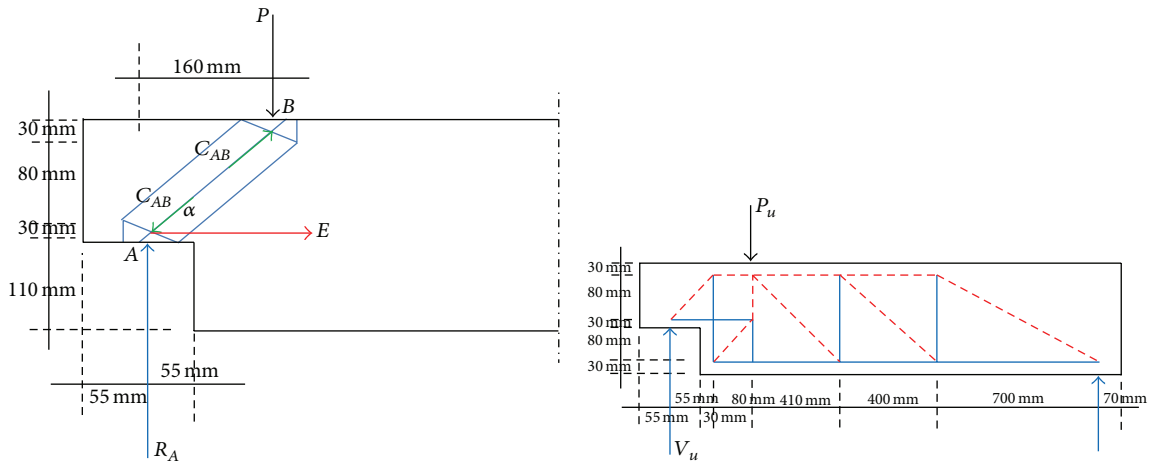

(a) Single node of truss model for DEB-1 and DEB-2

(b) STM for DEB-3 and DEB-4 (based on FIP model)

Figure 6: Truss model.

(4) diagonal tension in the nib

$$A_v = \frac{\left(V_u/\varphi - 2\lambda bd\sqrt{f_c'}\right)}{\left(2f_{yv}\right)}, \tag{5}$$

f_{yv} = the yield stress of vertical reinforcement in the nib.

The analysis results for the group of P^C using ACI code, RILEM provision, and PCI code are compared as shown in Table 3. According to failure load comparison, analysis using PCI code were found to be more accurate than ACI code and RILEM provision in predicting the failure load of RC-DEBs.

The common beams theory based on Bernoulli's theorem can not be applied to nonlinear condition and nonprismatic members in RC structures such as pile caps, deep beams, corbels, and dapped-end beams. STM provides an acceptable analysis and design solution for the nonlinear condition and disturbed regions subjected to high stress flow in RC structures [24, 25]. Many codes facilitate analysis using STM provisions. However, for STM analysis in this study, Eurocode2 [26] has been utilized.

As suggested by Mattock, trial and error has been conducted to select the most appropriate STM. The selected STM is consistent with the observed behavior of dapped-ends [8]. For DEB-1 and DEB-2, single node truss model has been used which consisted of one node-one strut-one tie at the support (CCT) as shown in Figure 6. For DEB-3 and DEB-4, truss model based on FIP provision has been used [27, 28].

For DEB-1 and DEB-2, node A is CCT. According to EC2 obtained,

$$\sigma_{Rd,\max} = k_2 \upsilon f_{cd}, \tag{6}$$

where $\sigma_{Rd,\max}$ is maximum design stress of RC beam, $k_2 = 0.85$ for CCT, $\upsilon = 1 - f_{ck}/250$, $f_{cd} = 0.567 f_{ck}$, f_{ck} is characteristic concrete compressive strength, and f_{cd} is design concrete compressive strength.

The analysis procedure is in accordance with the requirements of EC2. For DEB-1 and DEB-2, the single node truss model can accommodate their condition in which each DEB has no stirrup but only available nib flexure reinforcements (NFR). For DEB-3 and DEB-4, truss model established by FIP provision was used. Structure analysis of this truss model showed that internal force of hanger reinforcement is almost equal to the reaction force. This condition is in agreement with Mattock [8] suggestion. Results of analysis using STM are shown in Table 3.

For DEB-1, by using STM, the strength of strut is higher than tie so the failure load is determined by strength of tie (96.34 kN). Nib flexure reinforcements (tie) fail first. By comparing to experimental result, it can be seen that ACI code yields better result than STM for DEB-1 (56.25 kN). For DEB-2, by using STM, the failure load was also determined by strength of tie (96.34 kN). Meanwhile, by using RILEM provision, the failure load was 83.57 kN, so STM analysis provides better result than RILEM provision. For DEB-3 and DEB-4 as shown in Table 3, it can be seen that analysis results by using PCI code provide better results compared to STM analysis, ACI code, and RILEM provision.

Based on experimental results and by comparing to control beam (DEB-1), it had been found that the failure load increased by 51.93% by using engineered cementitious composite (ECC) in the dapped-end area, and the failure load increased by 62.26% and 46.69% as the amount of nib reinforcement and main flexural reinforcement increased, respectively.

The FEM analysis in this study was carried out by using Vec2. Each model uses a total of 687 elements which consist of rectangular element of 220, triangular element of 343, and truss element of 124 with total nodes of 452. For the analysis requirement, Vec2 uses elastic modulus of 28.6 KN/mm^2 and 22 KN/mm^2 for NSC and ECC, respectively. Poisson's ratio value of 0.15 and other parameters were used in accordance with the test specimen data. Analysis results are presented in Table 3.

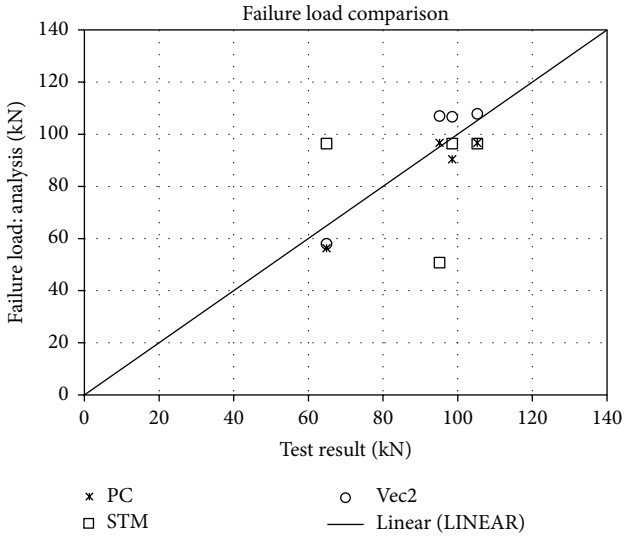

FIGURE 7: Dissemination of failure load values for experimental and analysis results.

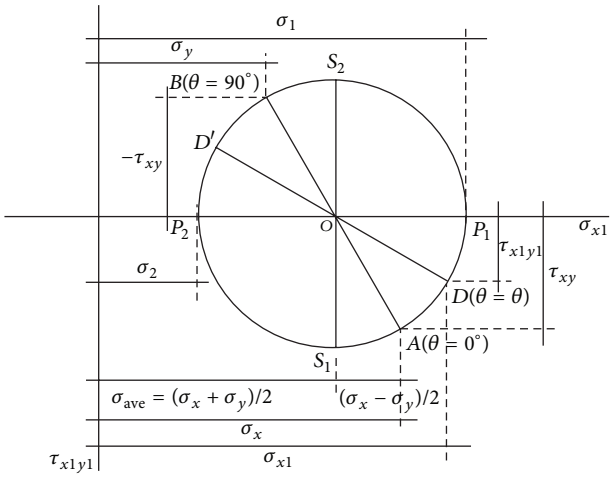

FIGURE 8: Mohr's circle.

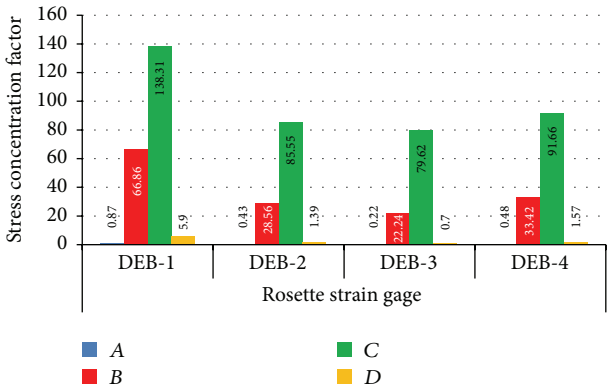

FIGURE 9: Stress concentration factor of RC-DEBs.

As shown in Table 3 and Figure 7, Vector2 analysis yields more accurate results than other methods as the finite element model in Vec2 can simulate the behavior of the RC-DEBs more realistically. All parameters related to the test specimen used were facilitated in Vec2 which involves concrete, steel reinforcements, the steel reinforcement configuration, section size of the test specimen, applied load and support position, and so forth. Based on input data, Vec2 had simulated all actual condition of the test specimens.

3.2. Stress Concentration. The intensity of a stress concentration is usually expressed by the ratio of the maximum stress to the nominal stress, called the stress concentration factor, k:

$$k = \frac{\sigma_1}{\sigma_{\text{nom}}}, \tag{7}$$

where $\sigma_{\text{nom}} = 80\%\ P_u/A_{cs}$ and A_{cs} is vertical shear plane area of dapped-end (same direction with reaction force). Figure 8 shows Mohr's circle, σ_1 denotes maximum principal stress, and σ_2 represents the minimum principal stress. The procedure on calculation of principal stresses is referred to Gere and Timoshenko [29].

The maximum principal stresses and stress concentration factor are shown in Table 4 and Figure 9. It is worth noting that the calculation is based on strain readings at 80% of the failure load to avoid any missing data due to damage of strain gage, suggested by Mohammed et al. [30]. From Table 4 and Figure 9 it can be observed that stress concentration factor for DEB-1 is higher than other beams and also stress concentration at point C is higher than other points of all beams. DEB-1 has the lowest failure load compared to other beams. Meantime stress concentration factor for DEB-3 is smaller than other beams and its stress concentration at point C is lower than other points of all beams. DEB-3 has the highest failure load compared to other beams. These observations presented that the value of stress concentration factor can indicate the failure load capacity of RC-DEBs. The highest stress concentration was found to occur at the reentrant corners.

3.3. The Failure Mode and Crack Pattern. The existence of recess (geometric discontinuity) in the end part of RC-DEB evokes the load path flow and raises the stress concentration at the vicinity of the reentrant corners leading to initiate cracks. According to experimental result, it showed that the first crack appears at the reentrant corner for all RC-DEBs. As the applied load increased, the principal tensile (maximum) stresses increased and the crack width also increased until final failure. It clearly indicates that the reentrant corner is the most susceptible to fail due to the applied load compared to another location of dapped-end area. Reentrant corner is the weakest point of RC-DEBs. This failure basically caused by the first crack initially propagates faster from the corner of the recess. As shown in (8), the strength capacity (moment capacity) of the nib is reduced due to the recessing in which the nib height is reduced and also the rigidity modulus (EI) of

Table 4: The principal stresses and stress concentration factor at each RC-DEB (for all types of strain gages).

DEB	Strain gage	80% of P_u KN	A_{cs} mm^2	σ_{nom} MPa	σ_2 MPa	σ_1 (σ_{max}) MPa	$k_i = \sigma_1/\sigma_{nom}$
DEB-1	A	51.78	16,800	3.08	(5.82)	2.67	0.87
	B	51.78	16,800	3.08	(147.62)	206.08	66.86
	C	51.78	16,800	3.08	(193.67)	426.29	138.31
	D	51.78	16,800	3.08	(12.88)	18.17	5.90
DEB-2	A	79.47	16,800	4.73	(5.26)	2.03	0.43
	B	79.47	16,800	4.73	(98.22)	135.11	28.56
	C	79.47	16,800	4.73	(171.14)	404.70	85.55
	D	79.47	16,800	4.73	(4.68)	6.57	1.39
DEB-3	A	84.07	16,800	5.00	(2.67)	1.12	0.22
	B	84.07	16,800	5.00	(79.30)	111.29	22.24
	C	84.07	16,800	5.00	(197.08)	398.42	79.62
	D	84.07	16,800	5.00	(0.64)	3.52	0.70
DEB-4	A	76.17	16,800	4.53	(5.17)	2.17	0.48
	B	76.17	16,800	4.53	(95.86)	151.54	33.42
	C	76.17	16,800	4.53	(160.55)	415.56	91.66
	D	76.17	16,800	4.53	(2.14)	7.12	1.57

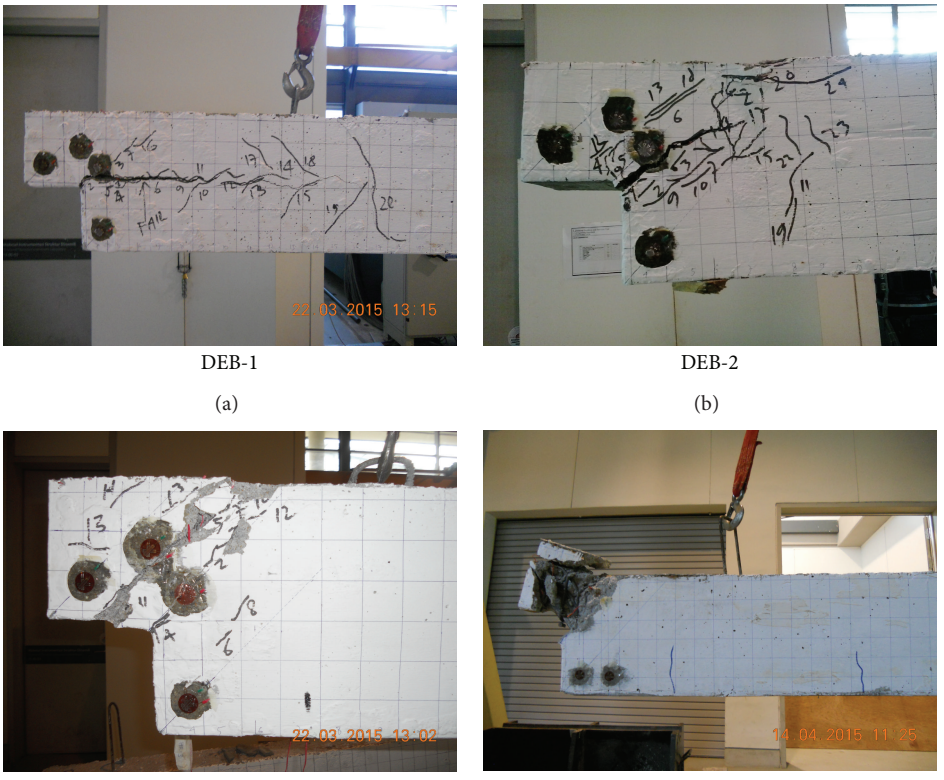

DEB-1 (a) DEB-2 (b) DEB-3 (c) DEB-4 (d)

Figure 10: Failure mode and crack pattern of test specimens.

Table 5: The deformation ratio between experimental and Vec2 analysis results.

Specimen	Experimental		Vector2		Vec2/Exp	
	$\delta^E{}_{max}$	$\delta^E{}_{rupt}$	$\delta^V{}_{max}$	$\delta^V{}_{rupt}$	$\delta^V{}_{max}/\delta^E{}_{max}$	$\delta^V{}_{rupt}/\delta^E{}_{rupt}$
	mm	mm	mm	mm	—	—
DEB-1	15.4	18.3	14.9	22.8	1.0	1.2
DEB-2	18.7	32.6	16.7	32.9	0.9	1.0
DEB-3	18.2	29.6	18.1	34.4	1.0	1.2
DEB-4	17.6	26.5	20.8	35.1	1.2	1.3
		Mean			1.0	1.2

δ_{max} = deflection of RC-DEB at maximum load condition; δ_{rupt} = deflection of RC-DEB at rupture condition.

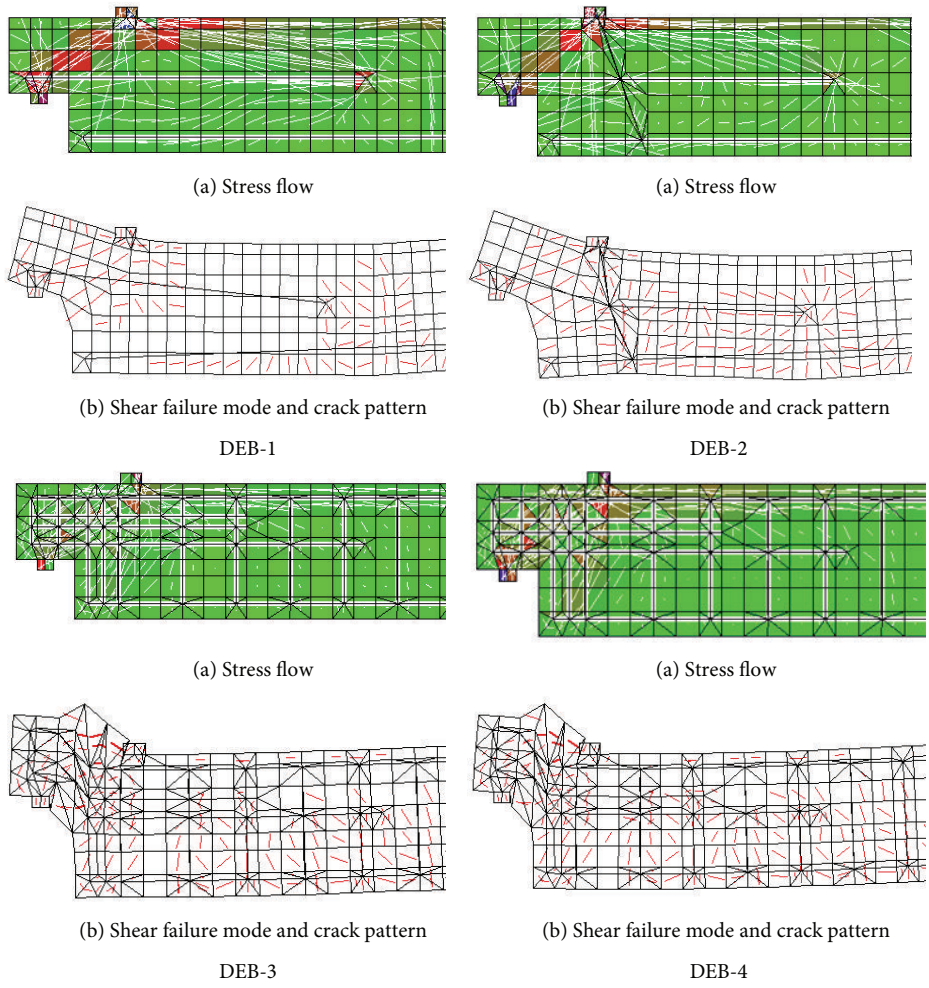

Figure 11: The high stress flow and crack pattern based on Vec2 analysis.

the nib between the reentrant corner and support is reduced as well [29]:

$$M = -EI\frac{d_y^2}{d_x^2}, \tag{8}$$

where M = nominal moment capacity, E = elastic modulus, I = inertia moment, and d_y^2/d_x^2 = the second-order differential of deflection.

Experimental results by Mohammed et al. [31] also demonstrated that presence of discontinuity leads to high stress concentrations at the corners of the opening which

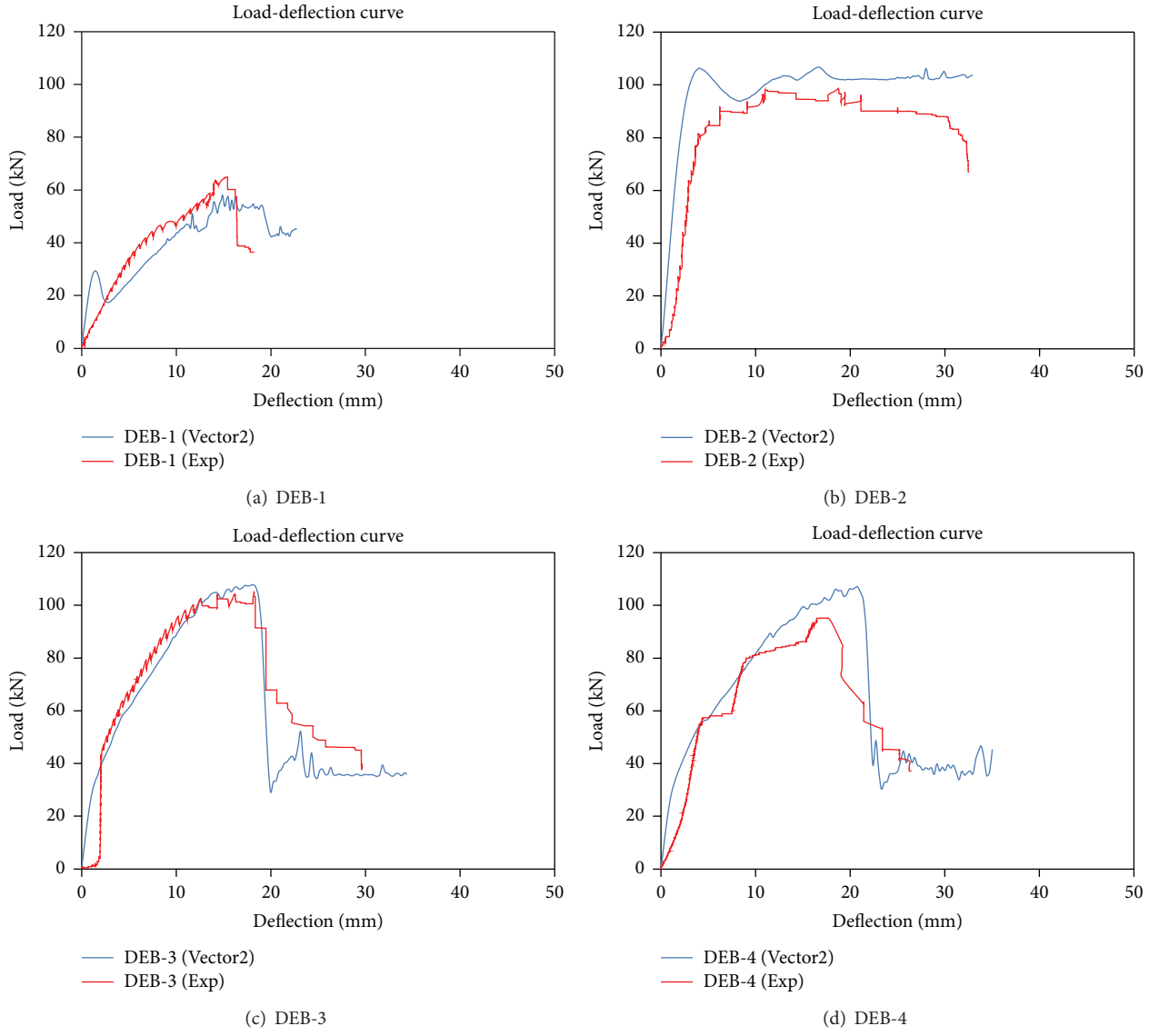

Figure 12: The load-deformation relationship.

initiates the cracks and leads to final failure. Mansur and Tan [32] stated that plastic hinges (yielding) also can occur at the region near the geometric discontinuity and it may cause the failure at this area.

Figure 10 shows the crack patterns of the tested beams. Unlike DEB-2, the bonding between concrete and steel reinforcements was weaker so that the shear crack propagating along the nib flexure reinforcement for DEB-1. ECC has the strong bonding with the steel reinforcement, so the crack propagation was not along the side of nib flexure reinforcements, but the cracks were propagating toward the loading point as shown in Figure 10. The tailoring of ECC (mechanical interactions between the fibers, matrix, and interface) can provide high performance of ECC even if the cracks width was wider. Therefore, ECC enhances strength capacity and ductility of RC-DEBs. For comparison, FEM Vec2 analysis which includes high stress flow and crack pattern of DEB models can be seen in Figure 11. Generally, the high stress flow and failure of RC-DEBs occur at the reentrant corners.

3.4. Load-Deformation Relationship. Comparison of load-deformation relationship between experimental and Vec2 analysis results was shown in Figure 12 and Table 5. The Vec2 analysis results are in good agreement with experimental results for all RC-DEBs. The mean value of the deformation ratio at maximum and rupture condition also present a good accuracy, where the ratio is close to 1. To obtain similar structural behavior of test specimen, Vec2 facilitates the appropriate model which involves concrete models, reinforcement models, and bond models. The concrete models cover compression prepeak and postpeak response, compression softening, tension stiffening and softening, tension splitting, confined strength, crack, and so forth, whereas

the reinforcement models cover hysteretic response, dowel action, and buckling. All these conditions had supported Vec2 for providing better accuracy of results than other analyses.

For requirement of tension stiffening model, in this Vec2 analysis uses modified Bentz 2003 [23]. Modified Bentz model proposes a tension stiffening formulation that involves the bond characteristics of the steel reinforcement, provided that the effect of tension stiffening relies upon dowel action after concrete cracked. The Vec2 models basically formulated for sectional analysis of reinforced concrete elements have been adapted by Vecchio and Wong [23] to consider for two-dimensional stress conditions and disposition of smeared and discrete reinforcement. All these conditions had supported Vec2 to provide better accuracy in predicting load-deformation than other analyses.

According to experimental results and by comparing to control beam (DEB-1), it had been also found that the failure deflection enhanced by 78.14% by using ECC in the dapped-end area, and the failure deflection enhanced by 61.75% and 44.81% as the amount of nib reinforcement and main flexural reinforcement increased, respectively. DEB-2 (the beam that uses ECC at the nib area) yields larger deflection capacity (32.6 mm) than other beams. Moreover, the failure load capacity of DEB-2 increased by 51.93% compared to DEB-1. So ECC provides better enhancement for strength capacity and ductility of RC-DEBs.

4. Conclusion

The following conclusions can be made from this study:

(1) Vec2 analysis provides better accuracy for predicting the failure load of RC-DEBs compared to other analysis approaches.

(2) The largest principal stress and the highest stress concentration factor of RC-DEBs occur at the reentrant corner and its vicinity, which potentially may indicate that the dominant cracks and failure occur at the reentrant corner of dapped-end.

(3) RC-DEBs which have the largest value of principal stress and stress concentration factor were the weakest as well as providing the lowest failure load capacity. RC-DEBs which have the smallest value of principal stress and stress concentration factor were the strongest as well as providing the highest failure load capacity.

(4) Vec2 analysis results are in good agreement with the experimental results in predicting the load-deformation response of the RC-DEBs.

(5) Using ductile engineered cementitious composite (ECC) at the dapped-end area of the beams will increase the strength capacity and plastic deformation.

(6) Reinforced dapped-end beams made of normal concrete usually fail in shear at the nib area. However, increasing the reinforcement ratio will enhance the strength capacity of these beams.

Conflict of Interests

The authors declare that there is no conflict of interests regarding the publication of this paper.

Acknowledgments

The authors would like to thank the Ministry of Education (MOE) of Malaysia and Universiti Teknologi PETRONAS for granting the project under codes FRGS 2013-2 and STIRF 38/2012, respectively.

References

[1] S. E.-D. F. Taher, "Strengthening of critically designed girders with dapped-ends," *Structures and Buildings*, vol. 158, no. 2, pp. 141–152, 2005.

[2] R. Herzinger, *Stud reinforcements in dapped-ends of concrete beams [Ph.D. thesis]*, University of Calgary, Calgary, Canada, 2008.

[3] W.-Y. Lu, I.-J. Lin, S.-J. Hwang, and Y.-H. Lin, "Shear strength of high-strength concrete dapped-end beams," *Journal of the Chinese Institute of Engineers*, vol. 26, no. 5, pp. 671–680, 2003.

[4] Q. Wang, Z. Guo, and P. C. J. Hoogenboom, "Experimental investigation on the shear capacity of RC dapped end beams and design recommendations," *Structural Engineering and Mechanics*, vol. 21, no. 2, pp. 221–235, 2005.

[5] A. H. Mattock and T. C. Chan, "Design and behavior of dapped end beams," *PCI Journal*, vol. 24, no. 6, pp. 28–45, 1979.

[6] P.-C. Huang and A. Nanni, "Dapped-end strengthening of full-scale prestressed double tee beams with FRP composites," *Advances in Structural Engineering*, vol. 9, no. 2, pp. 293–308, 2006.

[7] K.-H. Yang, A. F. Ashour, and J.-K. Lee, "Shear strength of RC dapped-end beams using mechanism analysis," *Magazine of Concrete Research*, vol. 63, no. 2, pp. 81–97, 2010.

[8] A. H. Mattock, *Strut-and-Tie Models for Dapped-End Beams*, Concrete International, 2012.

[9] T. Peng, *Influence of detailing on response of dapped-end beams [M.S. thesis]*, McGill University, Montreal, Canada, 2009.

[10] T. Nagy-György, G. Sas, A. C. Dâescu, J. A. O. Barros, and V. Stoian, "Experimental and numerical assessment of the effectiveness of FRP-based strengthening configurations for dapped-end RC beams," *Engineering Structures*, vol. 44, pp. 291–303, 2012.

[11] R. N. Mohamed and K. S. Elliot, *Shear Strength of Short Recess Precast Dapped-End Beams Made of Steel Fiber Self Compacting Concrete*, Singapore Concrete Institute, Singapore, 2008.

[12] H. Fukuyama, Y. Sato, V. C. Li, Y. Matsuzaki, and H. Mihashi, "Ductile engineered cementitious composite elements for seismic structural application," in *Proceedings of the World Conference on Earthquake Engineering (WCEE '00)*, 2000.

[13] V. C. Li and T. Kanda, "Engineered cementitious composites for structural applications," *Journal of Materials in Civil Engineering*, vol. 10, no. 2, pp. 66–69, 1998.

[14] M. D. Lepech and V. C. Li, "Large-scale processing of engineered cementitious composites," *ACI Materials Journal*, vol. 105, no. 4, pp. 358–366, 2008.

[15] E.-H. Yang and V. C. Li, "Tailoring engineered cementitious composites for impact resistance," *Cement and Concrete Research*, vol. 42, no. 8, pp. 1066–1071, 2012.

[16] H. M. E.-D. Afefy and M. H. Mahmoud, "Structural performance of RC slabs provided by pre-cast ECC strips in tension cover zone," *Construction and Building Materials*, vol. 65, pp. 103–113, 2014.

[17] J. Zhang, Z. Wang, X. Ju, and Z. Shi, "Simulation of flexural performance of layered ECC-concrete composite beam with fracture mechanics model," *Engineering Fracture Mechanics*, vol. 131, pp. 419–438, 2014.

[18] S. Qudah and M. Maalej, "Application of Engineered Cementitious Composites (ECC) in interior beam–column connections for enhanced seismic resistance," *Engineering Structures*, vol. 69, pp. 235–245, 2014.

[19] *PCI Design Handbook*, Precast/Prestressed Concrete Institute, 7th edition, 2010.

[20] A. Abid and K. B. Franzen, *Design of fiber reinforced concrete beams and slabs [M.S. thesis]*, Chalmers University of Technology, Gothenburg, Sweden, 2011.

[21] RILEM TC 162-TDF, "Test and design methods for steel fibre reinforced concrete," *Materials and Structures*, vol. 36, no. 262, pp. 560–567, 2000.

[22] ACI, "Building code requirements for structural concrete and commentary," ACI 318-08, 2008.

[23] F. J. Vecchio and P. S. Wong, *Vector2 & Formworks User's Manual*, University of Toronto, Toronto, Canada, 2002.

[24] A. Shah, E. Haq, and S. Khan, "Analysis and design of disturbed regions in concrete structures," *Procedia Engineering*, vol. 14, pp. 3317–3324, 2011.

[25] J. Schlaich and K. Schafer, "Design and detailing of structural concrete using strut and tie models," *The Structural Engineer*, vol. 69, no. 6, pp. 113–125, 1991.

[26] *Eurocode 2, Design of Concrete Structures, Part 1-1: General Rules and Rules for Buildings*, 2004.

[27] J. Y. Moreno-Martínez and R. Meli, "Experimental study on the structural behavior of concrete dapped-end beams," *Engineering Structures*, vol. 75, pp. 152–163, 2014.

[28] FIP Recommendations, *Practical Design of Structural Concrete*, CEB, FIP, 1999.

[29] J. M. Gere and S. P. Timoshenko, *Mechanics of Materials*, Stanley, Thornes (Publishers), 4th edition, 1999.

[30] B. S. Mohammed, L. W. Ean, and M. A. Malek, "One way RC wall panels with openings strengthened with CFRP," *Construction and Building Materials*, vol. 40, pp. 575–583, 2013.

[31] B. S. Mohammed, B. H. A. Bakar, and K. K. Choong, "Behaviour of axially loaded fired-claymasonry panels with openings," *The Indian Concrete Journal*, vol. 83, no. 4, pp. 9–16, 2009.

[32] M. A. Mansur and K. H. Tan, *Concrete Beams with Openings—Analysis and Design*, CRC Press, Boca Raton, Fla, USA, 1999.